Environ Earth Sci (2011) 64:1001–1010
DOI 10.1007/s12665-011-0918-y

ORIGINAL ARTICLE

Investigation of mercury levels in soil around a municipal solid waste incinerator in Shenzhen, China

Jun-Jian Wang · Hong-Wei Zhao · Xiu-Ping Zhong · Si-Fang Kong · Yang-Sheng Liu · Hui Zeng

Received: 26 February 2010 / Accepted: 10 January 2011 / Published online: 26 January 2011

Abstract Within the management hierarchy of municipal solid waste (MSW), incineration with energy recovery is a desired and viable option often used in densely populated and economically developed cities. The gaseous and particulate mercury (Hg) emitted from MSW incinerators may accumulate in the soil entering via dry and wet deposition. To investigate the soil Hg level and estimate the effects of the local meteorological and topographical characteristics (e.g., winds and terrain) on the soil Hg distribution, two layers of soil samples around an MSW incinerator in Shenzhen, China were collected and analyzed. Results showed that the Hg levels ranged from 0.012 to 0.136 mg kg^{-1} and from 0.013 to 0.100 mg kg^{-1} in the surface and subsurface soils, respectively. Long-term exposure of the soil to atmospheric Hg from the MSW incinerator dominates the spatial pattern of soil Hg. The wind frequency directly affected Hg distribution but not decisively. Interestingly, the variations of Hg level with downwind distance away from the stack were highly consistent with the terrain profile (r^2: 0.412–0.748). The effects of winds and terrain on soil Hg distribution and their mechanisms are discussed and general Hg dispersion patterns for transport on terrain are further proposed.

J.-J. Wang · H.-W. Zhao · X.-P. Zhong · S.-F. Kong · Y.-S. Liu (✉) · H. Zeng (✉)
College of Urban Planning and Design, Peking University, Shenzhen 518055, China
e-mail: yangshengliu@126.com

H. Zeng
e-mail: zengh@szpku.edu.cn

J.-J. Wang · H.-W. Zhao · X.-P. Zhong · S.-F. Kong · Y.-S. Liu · H. Zeng
Shenzhen Key Laboratory of Circular Economy, Shenzhen 518055, China

Keywords Hg · Municipal solid waste · Incineration · Soil · Terrain

Introduction

The environmental issues caused by mercury (Hg) and its compounds are of great concern because these chemicals are ubiquitous, highly toxic, persistent and bioaccumulative (Sheet 2004). Significant anthropogenic Hg sources include fossil fuel combustion (Yang and Wang 2008), municipal solid waste (MSW) incineration (Muenhor et al. 2009; Reis et al. 2007; Shaub 1993; Zemba et al. 1996), the chloralkali industry (Kinsey et al. 2004b; Southworth et al. 2005), fluorescent manufacturing (Clear and Berman 1994), battery manufacturing (Semu et al. 1986), pharmaceutical (Schilcher and Trittler 1997) and pesticide use (Primbs et al. 2008). Among these Hg sources, MSW incineration is commonplace in many regions including North America, Central and South America, Western Europe, and Africa, whereas Asia discharges the most via this route (Pirrone et al. 1996).

China is a major contributor to Hg discharge in environmental settlements in Asia brought about by its fast development in recent decades (United Nations Environment Programme Chemicals 2002). From 2003 to 2007, the annual amount of incinerated MSW in China has quadrupled to 14.3 million tons (National Bureau of Statistics of China 1996–2007). As MSW is collected without any source-separation requirements in China, items containing high levels of Hg enter MSW stream directly, such as batteries, fluorescent lamps, and thermometers. Approximately 96% of Hg in the MSW stream was estimated to be released as flue gas during incineration [24% in fly ash captured by the electrostatic precipitator (ESP), and 72% in

flue gas downstream ESP] (Brunner and Monch 1986). Most Hg is emitted into the atmosphere with flue gas or fly ash in toxic forms of Hg^0 and $HgCl_2$ (Carpi 1997). Not managed appropriately, the emissions from MSW incineration may impair both ecosystem and human health (Muenhor et al. 2009; Reis et al. 2007; Zemba et al. 1996).

Soil is an important sink for atmospheric Hg (Stein et al. 1996). About 48.2% of gaseous and particulate Hg in the atmosphere enters the soil or surface water via dry and wet deposition (Kaleri 2000). Though some fractions soon settle down and transform into stable form (e.g., HgS), they are potentially reduced by microbe metabolism and emigrate from soil (Wang et al. 1997). Investigating the soil Hg level is helpful to assess its role as a potential secondary pollution source through bioaccumulation into food chain (Cheng et al. 2006) or re-emitting into the bio-sensitive ground-level air (United States Environmental Protection Agency 1997). Further, Wang et al. (2003) observed a positive correlation between the atmospheric Hg concentration and the soil Hg content, which suggested that the soil Hg concentration may be an indicator to evaluate the atmospheric Hg pollution levels.

The Hg concentration in soil around MSW incinerators (MSWIs) has been previously reported in different regions (Llobet et al. 2002; Meneses et al. 1999; Nadal et al. 2005; Rimmer et al. 2006), with an observed maximum of 4.99 mg kg^{-1} in Newcastle, UK (Rimmer et al. 2006). Bache et al. (1991) found a significant correlation ($p = 0.01$) between the Hg concentrations in grass and the distance downwind from the stack, but subsequent work revealed anomalous observations on Hg distribution patterns (Llobet et al. 2002; Loppi et al. 2000). No consensus has been reached on the spatial pattern of Hg in soil. Moreover, it is assumed that the spatial pattern is dependent on the local terrain, but their relationship has not yet been investigated. In the present study, GPS data and local digital elevation model (DEM) are employed to quantify the effects of terrain.

The case-to-case distinctions of soil Hg patterns indicate different weights of input and output Hg fluxes, affected by processes such as atmospheric Hg transport and deposition, soil Hg loss by surface runoff, as well as soil Hg volatilization and percolation. The MSWI used in this study is in complex terrain, and thus the influencing processes may weigh far different. Gaussian plume model (GPM) is a basic plume dispersion model and most commonly used to predict atmospheric substance dispersion from point sources (Hanna et al. 1990; Katul et al. 2005; Meroney 1992). Exploring and analyzing the relationship between the Hg content in soil and that in ground-level air estimated by GPM can help to evaluate the long-term effect of atmospheric Hg dispersion.

The objectives of the paper are: (1) to identify the status of Hg pollution in two layers of soil around the selected MSWI and compare the results to other studies in different regions, (2) to compare Hg in soil with atmospheric Hg levels predicted by GPM, analyze the effects resulting from winds and terrain on Hg variability, and develop general Hg dispersion patterns.

Site description

Shenzhen is a fast developing and urbanizing city in the estuary of the Pearl River Delta, China. It has an annual temperature of ~23°C, annual precipitation ranging from ~1299 to ~2747 mm, and four distinct seasons. Based on Pasquill's (1974) theory, the local frequency distributions of atmospheric stability in classes B, D, E and F account for 16.0, 50.4, 11.6, and 17.1%, respectively (B unstable, C slightly unstable, D neutral stable, E slightly stable, F stable). East-southeast (ESE) winds are prevalent in summer while north-northeast (NNE) winds prevail in winter. The annual average wind velocity reaches 2.6 m s^{-1}.

Prior to 2005, the annual amount of local MSW has increased dramatically to 3.329 million tons (228 times that of year 1985) (Deng 2006), with more than 90% disposed via incineration in six MSWIs. The selected MSWI with processing load of 600 tons (MSW) per day and one stack of 60 m, located in central Shenzhen, has the longest history in China since its operation started in 1985. The fumes are treated by bag house filter and electrostatic precipitator, and then neutralized by lime and water in a wet scrubber before being discharged. In vicinity within 2 km from the stack, most western areas are undeveloped rolling mountains covered by subtropical forests, whereas the eastern areas are mainly residential districts covered mostly by hard concrete. According to the distribution map of mineralogical soil type in Shenzhen provided by Land and Resources Bureau of Shenzhen, the soil type of the study area (except the urbanized area) is yellow soil with low organic matter, formed from sand-shale. In the field work, low spatial heterogeneity of soil type was observed judged by soil profiles.

Materials and methods

Soil sampling and preparation

Four sampling lines are set (NNE, SES, WNW, and SSW) intersecting at the stack (Fig. 1), to estimate the influence of wind on the total Hg distribution in the research area. Surface soil (depth from 0 to 10 cm, designated as A) and subsurface soil (depth from 10 to 20 cm, designated as B) were both collected with a stainless steel spatula into PVC packages from each sample site that was within 2,000 m

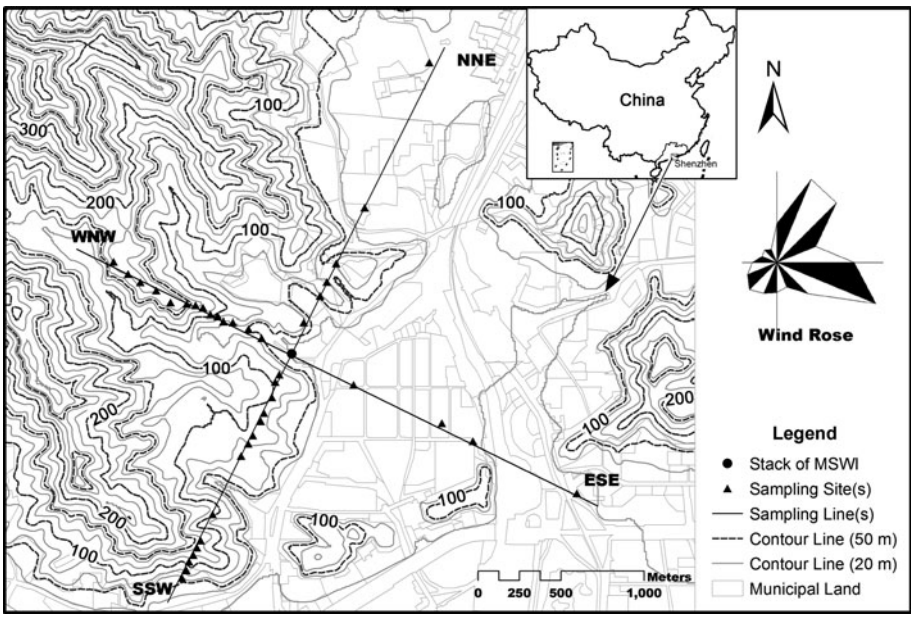

Fig. 1 Sampling distribution on the contour map

away from the stack on or closely beside the four sampling lines. Each sample was composed of five random fraction samples in a 3 × 3 m quadrant. The soils selected were mostly barren yellow soil, with pH range of 4.70–5.60, and organic matter range of 1.66–16.84 g kg^{-1}.

Rocks, non-decomposed roots, and residue from leaves were physically removed from the soil samples. All these samples were air dried in a shady, aerated and clean room until constant weight, then crushed by wooden stick, sieved through a 0.075 mm nylon sieve, and eventually stored in clean PVC bottles at 4°C before further process.

Analytical procedure

The dry sample (0.2 g) was treated with $H_2O_2/HNO_3/HCl$ (0.5, 6, and 2 mL, respectively) system and digested in Microwave Ethos 900 (Milestone, Italy). $SnCl_2$ (2%, w/v) in HCl solution (4%, v/v) was used as redundant, and Hg in the soil samples was determined in dry weight by cold vapor atomic absorption (FIMS 400, Perkin Elmer, US, detection limit <0.01 μg/L). The blank and the standard substances were simultaneously determined. Reference material (geochemical standard reference sample soil in China, GSS-6) and standard solution ($Hg(NO_3)_2$) were used for quality control and quality assurance. The recovery values ranged as 90.2–102.7, 88.8–98.5%, respectively. The means of no less than three replicate analyses were presented as result.

Data visualization

GPM (Pasquill 1974) was employed to calculate the atmospheric C_{Hg} at ground level. The estimated mercury concentration in air—C_{Air} at location (x, y, z) downwind from a source in ng m^{-3} is calculated as

$$C_{Air} = \frac{Q}{2\pi u \sigma_y \sigma_z} \times \exp\left[-0.5\left(\frac{y}{\sigma_y}\right)^2\right] \times \left\{\exp\left[-0.5\left(\frac{z-H}{\sigma_z}\right)^2\right] + \exp\left[-0.5\left(\frac{z+H}{\sigma_z}\right)^2\right]\right\} \quad (1)$$

where x, y and z the coordinates that define the location (m), Q pollutant emission rate (ng m^{-3}), u average wind speed (m s^{-1}), σ_y y direction plume standard deviation (m), σ_z z direction plume standard deviation (m), H effective stack height (m).

We calculated σ_y and σ_z according to Martin's (1976) estimate:

$$\sigma_y = ax^b \quad (2)$$

$$\sigma_z = cx^d + f \quad (3)$$

where x downwind distance (km), a, b, c, d and f constants differ by atmospheric stability.

For the calculations, the neutral atmospheric stability (class D) was selected. Then the effective stack height and the plume rise were estimated according to the equations below (Aarne Vesilind et al. 1994):

$$H = h_{physical} + \Delta h \quad (4)$$

$$\Delta h = 3.47\frac{V_s d_H}{u} + 5.15\frac{\sqrt{Q_h}}{u} \quad (5)$$

where $h_{physical}$ y direction plume standard deviation (m), Δh plume rise (m), V_s stack gas exit velocity (m s^{-1}), d_h stack diameter (m), Q_h stack heat emission rate (kJ s^{-1}).

DEM of local area with cell size of 10 × 10 m was adopted and calculated based on ArcGIS Version 9.2 to visualize the Hg dispersion by GPM. Isotropic wind velocity of 2.6 m s^{-1} was adopted in visualization while anisotropic averages wind velocities of the four directions were used for statistical analysis.

Geostatistics is useful in both characterizing spatial variability and mapping a variety of soil properties (Yang and Wang 2008). The Hg concentrations of surface and subsurface soils (both accorded with normal distribution, $p < 0.01$) were both visualized on map by ordinary Kriging. The best fit isotropic variogram models (Gaussian model for surface soil with r^2 of 0.403 and proportion of *partial sill* to *sill* of 0.944, spherical model for subsurface soil with r^2 of 0.429, proportion of *partial sill* to *sill* of 0.733) were calculated and determined by software GS+ Version 9. Though the samples were not evenly distributed so that the accuracy of prediction was questionable, trends on four sampling lines were significant in two interpolated maps to compare with the result of GPM prediction.

Statistical analysis

The level of significance for all tests was fixed at 0.05. All statistical analyses were done using SPSS version 16.0.

Results

Mercury levels in the soils of 0–10 cm and 10–20 cm

The Hg concentrations in surface soil (noted as C_A 0.012–0.136 mg kg^{-1}, with the mean at 0.058 mg kg^{-1}) and subsurface soil (noted as C_B 0.013–0.100 mg kg^{-1}, with the mean at 0.050 mg kg^{-1}) are reported in Table 1. Considering the directions, the range of C_A in NNE was 0.030–0.115 mg kg^{-1}; in ESE, 0.019–0.040 mg kg^{-1}; in SSW, 0.012–0.097 mg kg^{-1}; and in WNW, 0.016–0.136 mg kg^{-1}. That of C_B in NNE was 0.016–0.082 mg kg^{-1}; in ESE, 0.017–0.052 mg kg^{-1}; in SSW, 0.015–0.084 mg kg^{-1}; and in WNW, 0.018–0.100 mg kg^{-1}. The observed mean Hg concentration was slightly higher

Table 1 Comparison of mercury concentrations in study area and around other MSW/HWI(s) reported in literatures

References	MSWI/HWI				Sampling				C_{Hg}[a] (mg kg^{-1}, except aerosol in ng m^{-3})		
	Location	Scale (t $year^{-1}$)	Started	Stack height (m)	Media	Distance from stack (km)	Depth for soil (cm)	Number	Range	Median	Mean
This study	Shenzhen, China	219,000	1985	60	Soil	≤2	0–10	40	0.012–0.136	0.058	0.058
							10–20	40	0.013–0.100	0.054	0.050
Bache et al. 1991	US	40,150	1983	25	Herbage	≤0.9	NA	20	0.00–0.20	0.04	0.06
Meneses et al. 1999	Montcada, Spain	45,000	1975	45	Soil	≤3	0–3	24	NA	NA	0.09 (1996)
											0.11 (1997)
					Herbage	≤3	NA	24	NA	NA	0.05 (1996)
											0.12 (1997)
Loppi et al. 2000	Tuscany, central Italy	14,400	1996	30	Herbage	≤10	NA	11	0.082–0.177	0.136	0.134
Llobet et al. 2002	Catalonia, Spain	140,000	1991	NA	Soil	≤1.5	0–3	24	NA	NA	0.06 (1994)
											0.08 (1997)
											0.05 (1999)
					Herbage	≤1.5	NA	24	NA	NA	0.07 (1994)
											0.02 (1997)
											0.10 (1999)
Hu et al. 2003	Taiwan	109,500	NA	120	Aerosol	≤3.5	NA	8	0.07–13	0.095	1.7
Nadal et al. 2005	Catalonia, Spain	NA	NA	55	Soil	≤7	0–3	40	NA	NA	0.16 (1998)
											0.08 (2003)
					Herbage	≤7	NA	40	NA	NA	0.23 (1998)
Rimmer et al. 2006	Newcastle, UK	NA	NA	NA	Soil	≤2.25	0–5	163	0.03–4.99	0.32	0.50
Muenhor et al. 2009	Samui Island, Thailand	51,100	2001	59	Soil and sediment	≤5	0–15	83	0.076–0.275	NA	NA
							15–25				
							25–40				

NA not available

[a] Differences in the Hg concentrations could be due to differences in media used for comparison or/and different methodologies applied in each study used for comparison. Comparison between different media should be avoided since mercury behaves differently in each medium

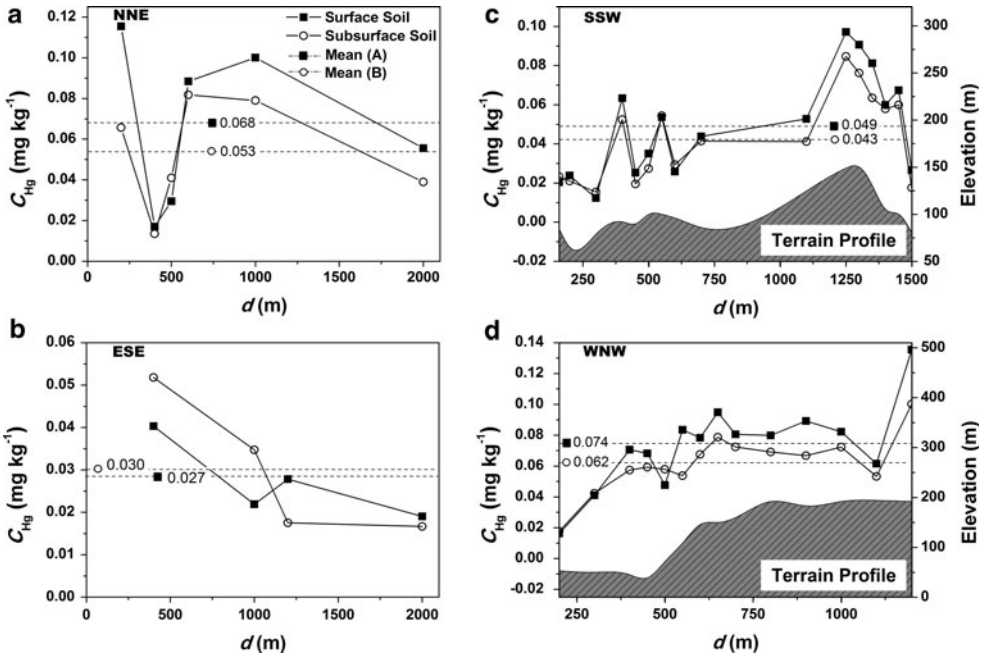

Fig. 2 Mercury distribution with increasing distance downwind from the stack (*d*) on the four sampling lines

compared with the previously reported mean concentration of Hg in natural yellow soil from Shenzhen at 0.044 mg kg^{-1} (Tao and Deng 1993). C_A and C_B differ significantly ($p < 0.001$) and have a significant linear correlation ($r^2 = 0.880$). 77.5% of all paired samples had a ratio of $C_B/C_A \leq 1$, indicating remarkable dissipation with increasing depth in samples sites on gently slope. At the 0.05 level, the percentage of mercury concentration diminishing from surface soil to subsurface soil (8.90% ± 21.2%) was significantly drawn from a normally distributed population by K–S normality test and the highest probability was 7.36%.

Figure 2 illustrates the variations of C_A and C_B with the downwind distance (*d*) away from the stack in four sampling directions: NNE, ESE, SSW, and WNW. The variations differed from each other in these directions, and only the Hg levels in the ESE presented a decreasing trend with an increase of *d*, consistent with the results observed by Bache et al. (1991). Statistical result (Fig. 3) suggested that the WNW was the most polluted area probably due to the highest frequency of the ESE winds and the flat terrain in eastern area. The average values of C_A (or C_B) were decreased in the four directions following such order: WNW > NNE > SSW > ESE (Figs. 2, 3). However, the wind rose showed that the corresponding wind frequencies in the four directions were decreased in the following order: ESE winds > NNE winds > SSW winds > WNW winds (Fig. 3). Therefore, the spatial distribution of Hg in the four directions was not fully consistent with the strength of the wind frequency.

Mercury contamination around MSWIs from references are also summarized (Table 1). The soil Hg

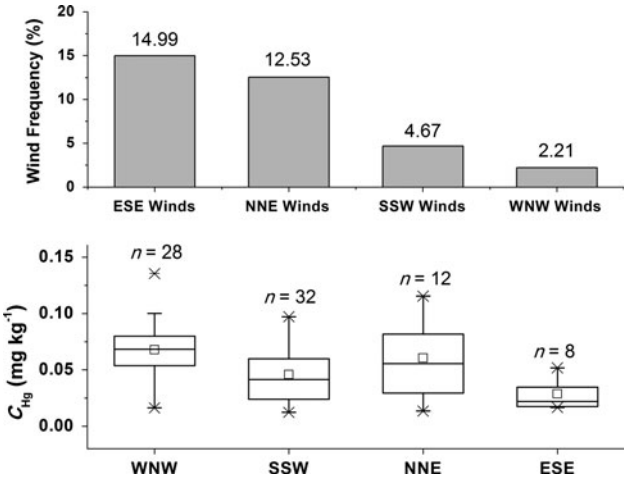

Fig. 3 Wind frequencies of the four directions and corresponding *box charts* of the mercury concentrations in the downwind areas

concentration varied with a wide range in different studies, with the means ranging from 0.05 to 0.50 mg kg^{-1}. Compared with the previous literatures, the MSWI in the present study has the largest disposal scale and the second longest operation duration only following that in Montcada, Spain (Meneses et al. 1999), but results indicated that the soil Hg concentrations in this study were relatively low.

Relationship of the local terrain and the Hg concentration in forest soil

The lands in the SSW and WNW areas are covered by natural forest without obvious signs of human exploitation.

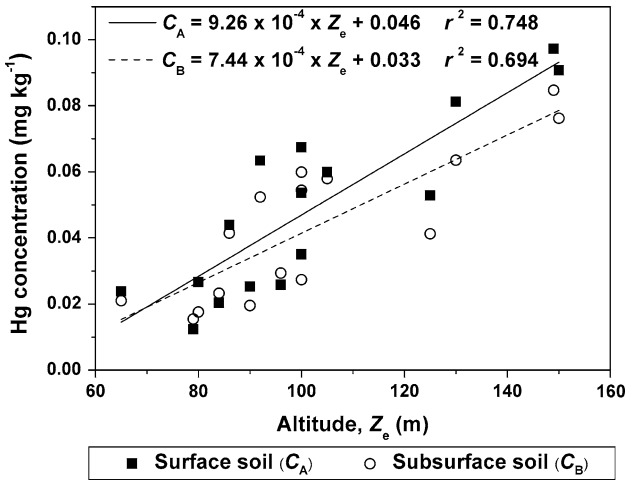

Fig. 4 Linear regressions of the mercury concentrations of surface and subsurface soils (C_A and C_B) versus the sampling elevation (Z_e) in the SSW area

As shown in Fig. 2, the variation trends of C_A and C_B with an increase of downwind distance were roughly consistent with the terrain profile, which was drawn according to the elevation of sampling sites measured by GPS. In the SSW area, the coefficient of determination from linear regression between C_A and the elevation was $r^2 = 0.748$ ($p < 0.001$), and that between C_B and the elevation was $r^2 = 0.694$ ($p < 0.001$) (Fig. 4). As to the WNW area, the correlations were weaker but still significant (r^2: 0.412–0.416, $p_A = 0.013$, $p_B = 0.013$), which can probably be ascribed to the less complicated terrain and lower change in elevation of the sampling site.

Relationship of Hg in soil and ground-level air predicted by GPM

The C_{Air} at ground level corresponding with the sampling sites was calculated using the individual average wind velocities of the four directions. C_{Air} varied from 0 to 0.648 ng m^{-3}, with the mean at 0.084 ng m^{-3}. It was slightly lower than the Hg concentration in aerosol determined by Hu et al. (2003) (Table 1). By the comparisons of both C_A and C_B in forest soil (in the WNW and SSW areas) with C_{Air}, respectively, correlations were found significant but weak ($p_A = 0.004$, $p_B = 0.003$, $n = 30$). The Hg concentration in ground-level air calculated by GPM is also presented (Fig. 5a) with kriging prediction maps of C_A and C_B (Fig. 5b, c). It was noted that the Hg concentration in three maps presented a consistent trend in forested areas. As to the urban areas (NNE and ESE areas), significant correlation between the soil Hg concentration (C_A or C_B) and C_{Air} was not observed.

Discussion

Importance of various factors affecting soil Hg distribution

The major Hg input to the soil was suspected from the atmospheric Hg released by the MSWI, and is confirmed by the consistency of Hg distribution in forest soil with that in air estimated by GPM. GPM takes limited variables into account so that it is hardly sufficient for accurate quantitative prediction. Hg exchange between air and soil surface

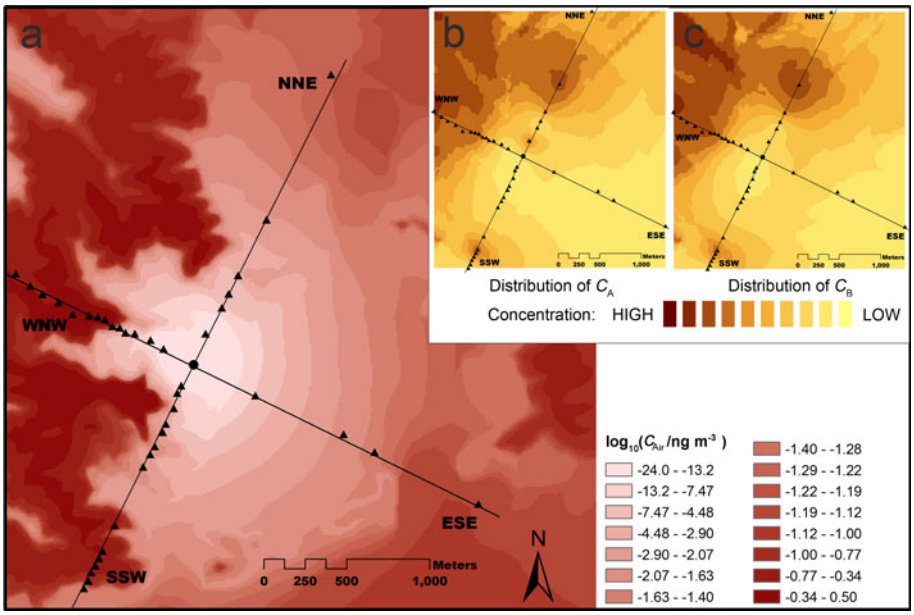

Fig. 5 Comparison of C_{Air} predicted by GPM with trends of C_A and C_B by ordinary kriging: **a** distribution of C_{Air}—estimated ground-level mercury concentration in air, **b** distribution of C_A—mercury concentration in surface soil, and **c** distribution of C_B—mercury concentration in subsurface soil

is going on at all times (Bahlmann et al. 2006; Xin and Gustin 2007). The air–soil partitioning of Hg is readily influenced by other factors such as dry and wet deposition, soil loss, variation of the soil characteristics, and human intervention in a specific case. All these factors are beyond GPM's estimation so that C_{Air} had a weak correlation with C_A (or C_B). Despite these shortcomings, the significant correlations reveal that the atmospheric Hg dispersion and deposition processes (input) dominate the soil Hg spatial pattern around an MSWI. Consequently, the local meteorological and topographic characteristics, as important factors in air dispersion, inevitably affect the soil Hg distribution.

The differences between Hg concentrations in surface and subsurface soils were generally regarded as the result of Hg deposition and infiltration process. The physicochemical mechanisms of Hg dissipation causing these differences were available in some previous studies (Amirbahman et al. 2002; Brandon et al. 2001; Gillis and Miller 2000; Slowey et al. 2005). It was well documented that the Hg could be adsorbed/bound to soil organic matter (SOM) causing Hg retention during its infiltration. Therefore, the surface soils which contained more SOM had higher Hg concentrations. But herein the soil Hg concentration and SOM were not significant correlated ($p > 0.1$), suggesting that strong external interference, e.g., Hg deposition, may have broken the adsorption equilibrium.

The output from soil decreased the soil Hg level. The observed Hg concentrations were somewhat lower than those of other MSWIs listed in Table 1, probably due to the sampling methods and occurrence of soil erosion. It may be influenced by sampling depth (0–10, 10–20 cm herein versus 0–3 or 0–5 cm in previous researches) as shown in this study where significant dissipation from surface soil to subsurface soil took place. Importantly, low pH is not favorable to Hg adsorption for its strong desorption ability (Semu et al. 1987). In this case, the low soil pH (4.70–5.60) can significantly reduce Hg retention in the soil.

Effects of wind

Wind is an important factor in atmospheric Hg dispersion (Carpi et al. 1994). Theoretically, the wind frequency determines the accumulated Hg amount in downwind direction, whereas the wind velocity affects the atmospheric dispersion distance. However, the spatial distribution of Hg concentrations does not correlate as well with wind frequency or wind velocity in this study as shown in other studies (Llobet et al. 2002; Meneses et al. 1999; Rimmer et al. 2006; Schuhmacher et al. 1997). It is difficult to evaluate the pollution levels in different directions simply according to the winds, especially in a small local area where the turbulence, velocity and direction of the wind can be easily changed by terrain or thermal instability resulting from scattered small heat sources. The other small non-point Hg sources present in the study area (e.g., fossil fuel combustion for travel purposes or heating residencies in the urban section), though not focused on, might also have contributed to the spatial distribution of soil Hg. Nevertheless, the lower Hg concentration in the SSW than that in the NNE (see in Fig. 3) may be attributable to the fact that the NNE winds have the strongest wind velocity (3.5 m s^{-1} on annual average), and thus Hg has dispersed even further than the study region in the SSW.

Effects of terrain

Compared to wind, physical features of the land appear to affect the Hg distribution the most in uneven obstructed terrain. As illustrated in Fig. 4, the Hg concentration in soil is likely a function of elevation. Its internal mechanism consists of multiple factors. Generally speaking, the Hg distribution can be affected by four factors:

1. obstruction effects, which alter properties of the wind and deviate plume from original centerline, and the airborne pollutants thus migrate,
2. slope effects, which accelerate the soil erosion and lower the Hg concentration in soil, thus altering the soil adsorption ability of ground-level air as well (Xin and Gustin 2007),
3. conflux effects, which enhance the moisture of soil that has been proved to favor Hg emissions from soil (Gustin and Stamenkovic 2005), and
4. shade effects, which shelter soil from sunlight, especially from UV, factors inducing Hg redox reactions (Xin et al. 2007; Zhang and Lindberg 1999); and which cause the difference of soil temperature affecting the air–soil partitioning (Zhang et al. 2001).

Results of the present study have provided evidence for the former two effects (obstruction and slope effects): The C_{Hg} rose on the windward slope and decreased on the leeward slope, particularly in SSW direction; the sampling sites at steeply surface (slope $> 50°$) including NNE500, NNE600, SSW300, SSW1400, and WNW500 had lower ratios of C_A to C_B compared to nearby sampling sites (Fig. 2). However, the other effects lack data to be proved in this investigation. A series of simulated experiments and tests on these four effects are going on in our group.

General Hg dispersion patterns

Variability of the Hg concentration with downwind distance determines the spatial pattern of Hg distribution. But the influence of downwind distance on the Hg concentration is uncertain and conflicting. Bache et al. (1991)

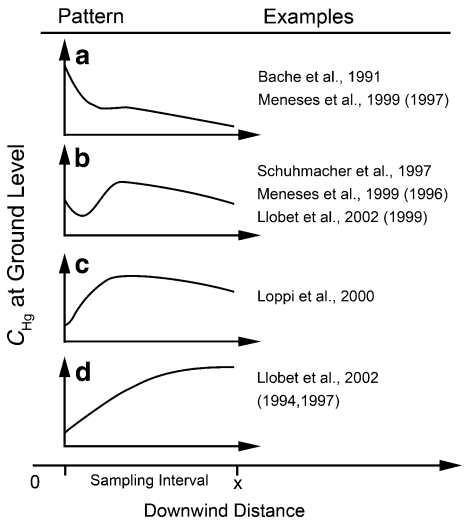

Fig. 6 Four proposed patterns for mercury dispersion to ground level on relative flat terrain around an MSWI: **a** strong fugitive effect, **b** neutral fugitive effect, **c** weak fugitive effect with slight wind and **d** weak fugitive effect with strong wind. All four of them showed rough trends instead of exact functions

observed a decreasing concentration trend which was contrary to the results of 1994 and 1997 reported by Llobet et al. (2002). Other literature also revealed irregular trends (Loppi et al. 2000; Semu et al. 1987). If all Hg comes from the single stack discharge, the spatial patterns of Hg should be similar when the terrain is even. However, the fugitive emissions from processing and storage areas in the MSW incineration plant, where the indoor Hg concentration can even exceed 1,000 ng m^{-3} (Liu et al. 2009), can influence the spatial pattern of atmospheric Hg remarkably. The fugitive emissions from MSW incineration plant were seldom investigated, but that from chloralkali industry has a strong influence on the surrounding soil within hundreds of meters and the Hg concentration decreased rapidly with distance (Kinsey et al. 2004a; Southworth et al. 2004).

Under ideal conditions without interference, the Hg spatial pattern would still be diverse under different strengths of the stack effect and those of the fugitive effect, depending on disposal scale, technique, instrument and management of the MSWI. If most of the atmospheric Hg comes from both fugitive emissions and stack emissions, the spatial pattern can be understandable. Four patterns of Hg dispersion are proposed for transport on terrain (at ground level) in relatively even area resulting from strong fugitive effects to weak, and the observations from previous researches are also classified (Fig. 6). This hypothesis helps explain the "irregular trends" observations in their studies. It is probable that most Hg distribution around MSWI at ground level would correlate with these four patterns approximately, but there are still many factors to distract it from the estimate, especially local meteorological and topographic conditions as mentioned.

Conclusion

In this study, the atmospheric Hg dispersion from MSWI dominates the spatial pattern of surrounding soil Hg. The dispersion process is dependent on downwind distance that the previous research has similarly shown, as well as winds and terrain that this study focused on, but none is able to predict the Hg concentration individually. Based on the previous work and this study, four general Hg dispersion patterns for transport on the terrain considering both stack discharge and fugitive emissions have been hypothesized. However, the complicated environmental factors make them hard to be examined and further simulations and tests are necessary.

Acknowledgments This research was financially supported by the National Natural Science Foundation of China (Grant 20877002), and the "Shenzhen Double-Hundred Talents" program. Thanks the Shenzhen Environmental Monitoring Centre for assistance in instrument analysis. The authors are also grateful to Ying-Han Li for help on sampling and Prof. Eugene Leong for help on language improving.

References

Aarne Vesilind P, Jeffrey Peirce J, Weiner RF (1994) Environmental engineering. Butterworth Heinemann, Woburn

Amirbahman A, Reid AL, Haines TA, Kahl JS, Arnold C (2002) Association of methylmercury with dissolved humic acids. Environ Sci Technol 36(4):690–695

Bache CA, Gutenmann WH, Rutzke M, Chu G, Elfving DC, Lisk DJ (1991) Concentrations of metals in grasses in the vicinity of a municipal refuse incinerator. Arch Environ Contam Toxicol 20(4):538–542

Bahlmann E, Ebinghaus R, Ruck W (2006) Development and application of a laboratory flux measurement system (LFMS) for the investigation of the kinetics of mercury emissions from soils. J Environ Manage 81(2):114–125

Brandon NP, Francis PA, Jeffrey J, Kelsall GH, Yin Q (2001) Thermodynamics and electrochemical behaviour of Hg-S-Cl-H2O systems. J Electroanal Chem 497(1–2):18–32

Brunner PH, Monch H (1986) The flux of metals through municipal solid-waste incinerators. Waste Manage Res 4(1):105–119

Carpi A (1997) Mercury from combustion sources: a review of the chemical species emitted and their transport in the atmosphere. Water Air Soil Pollut 98(3–4):241–254

Carpi A, Weinstein LH, Ditz DW (1994) Bioaccumulation of mercury by sphagnum moss near a municipal solid-waste incinerator. J Air Waste Manage 44(5):669–672

Cheng JP, Yuan T, Wang WH, Jia JP, Lin XY, Qu LY, Ding ZH (2006) Mercury pollution in two typical areas in Guizhou province, China and its neurotoxic effects in the brains of rats fed with local polluted rice. Environ Geochem Health 28(6): 499–507

Clear R, Berman S (1994) Environmental and health-aspects of lighting—mercury. J Illum Eng Soc 23(2):138–152

Deng P (2006) Shenzhen statistical yearbook. China Statistical Publishing House, Beijing
Gillis AA, Miller DR (2000) Some local environmental effects on mercury emission and absorption at a soil surface. Sci Total Environ 260(1–3):191–200
Gustin MS, Stamenkovic J (2005) Effect of watering and soil moisture on mercury emissions from soils. Biogeochemistry 76(2):215–232
Hanna SR, Chang JS, Strimaitis DG (1990) Uncertainties in source emission rate estimates using dispersion models. Atmos Environ 24(12):2971–2980
Hu CW, Chao MR, Wu KY, Chang-Chien GP, Lee WJ, Chang LW, Lee WS (2003) Characterization of multiple airborne particulate metals in the surroundings of a municipal waste incinerator in Taiwan. Atmos Environ 37(20):2845–2852
Kaleri CJ (2000) Implementation issues: mercury transport & fate combustion risk assessments in region 6. US EPA, Region. http://www.epa.gov/earth1r6/6pd/rcra_c/pd-o/mercury2.pdf. Accessed December 2009
Katul GG, Porporato A, Nathan R, Siqueira M, Soons MB, Poggi D, Horn HS, Levin SA (2005) Mechanistic analytical models for long-distance seed dispersal by wind. Am Nat 166(3):368–381
Kinsey JS, Anscombe FR, Lindberg SE, Southworth GR (2004a) Characterization of the fugitive mercury emissions at a chlor-alkali plant: overall study design. Atmos Environ 38(4):633–641
Kinsey JS, Swift J, Bursey J (2004b) Characterization of fugitive mercury emissions from the cell building at a US chlor-alkali plant. Atmos Environ 38(4):623–631
Liu YS, Zhan ZY, Du F, Kong SF, Liu YS (2009) Indoor air concentrations of mercury species in incineration plants for municipal solid waste (MSW) and hospital waste (HW). Chemosphere 75(2):266–271
Llobet JM, Schuhmacher M, Domingo JL (2002) Spatial distribution and temporal variation of metals in the vicinity of a municipal solid waste incinerator after a modernization of the flue gas cleaning systems of the facility. Sci Total Environ 284(1–3): 205–214
Loppi S, Putorti E, Pirintsos SA, De Dominicis V (2000) Accumulation of heavy metals in epiphytic lichens near a municipal solid waste incinerator (Central Italy). Environ Monit Assess 61(3): 361–371
Martin DO (1976) Comment on "The change of concentration standard deviations with distance". J Air Pollut Control Assoc 26:145–147
Meneses M, Llobet JM, Granero S, Schuhmacher M, Domingo JL (1999) Monitoring metals in the vicinity of a municipal waste incinerator: temporal variation in soils and vegetation. Sci Total Environ 226(2–3):157–164
Meroney RN (1992) Dispersion in non-flat obstructed terrain and advanced modeling techniques. Plant Oper Program 11(1):6–11
Muenhor D, Satayavivad J, Limpaseni W, Parkpian P, Delaune RD, Gambrell RP, Jugsujinda A (2009) Mercury contamination and potential impacts from municipal waste incinerator on Samui Island, Thailand. J Environ Sci Heal A 44(4):376–387
Nadal M, Bocio A, Schuhmacher M, Domingo JL (2005) Trends in the levels of metals in soils and vegetation samples collected near a hazardous waste incinerator. Arch Environ Contam Toxicol 49(3):290–298
National Bureau of Statistics of China (1996–2007) China statistical yearbook. China Statistical Publishing House, Beijing
Pasquill F (1974) Atmospheric diffusion. Wiley, New York
Pirrone N, Keeler GJ, Nriagu JO (1996) Regional differences in worldwide emissions of mercury to the atmosphere. Atmos Environ 30(17):2981–2987
Primbs T, Wilson G, Schmedding D, Higginbotham C, Simonich SM (2008) Influence of Asian and Western United States agricultural areas and fires on the atmospheric transport of pesticides in the Western United States. Environ Sci Technol 42(17):6519–6525
Reis MF, Sampaio C, Brantes A, Aniceto P, Melim M, Cardoso L, Gabriel C, Simao F, Miguel JP (2007) Human exposure to heavy metals in the vicinity of Portuguese solid waste incinerators—Part 1: biomonitoring of Pb, Cd and Hg in blood of the general population. Int J Hyg Environ Health 210(3–4):439–446
Rimmer DL, Vizard CG, Pless-Mulloli T, Singleton I, Air VS, Keatinge ZAF (2006) Metal contamination of urban soils in the vicinity of a municipal waste incinerator: one source among many. Sci Total Environ 356(1–3):207–216
Schilcher H, Trittler R (1997) Investigations on the evaluation of mercury residues in medicinal plants, plant drugs and plant drug preparations. 4. On hazardous contaminant contents in plant drugs and drug preparations. Pharm Ind 59(1):90–94
Schuhmacher M, Meneses M, Granero S, Llobet JM, Domingo JL (1997) Trace element pollution of soils collected near a municipal solid waste incinerator: human health risk. Bull Environ Contam Toxicol 59(6):861–867
Semu E, Singh BR, Selmerolsen AR (1986) Mercury pollution of effluent, air, and soil near a battery factory in Tanzania. Water Air Soil Poll 27(1–2):141–146
Semu E, Singh BR, Selmerolsen AR (1987) Adsorption of mercury-compounds by tropical soils. 2. Effect of soil-solution ratio, ionic-strength, pH, and organic-matter. Water Air Soil Poll 32(1–2):1–10
Shaub WM (1993) Mercury emissions from MSW incinerators—an assessment of the current situation in the United-States and forecast of future emissions. Resour Conserv Recyl 9(1–2):31–59
Sheet E (2004) National listing of fish advisories. United States Environmental Protection Agency, Office of Water. http://www.epa.gov/waterscience/fish/advisories/factsheet.pdf. Accessed December 2009
Slowey AJ, Rytuba JJ, Brown GE (2005) Speciation of mercury and mode of transport from placer gold mine tailings. Environ Sci Technol 39(6):1547–1554
Southworth GR, Lindberg SE, Zhang H, Anscombe FR (2004) Fugitive mercury emissions from a chlor-alkali factory: sources and fluxes to the atmosphere. Atmos Environ 38(4):597–611
Southworth GR, Lindberg SE, Bogle MA, Zhang H, Kuiken T, Price J, Reinhart D, Sfeir H (2005) Airborne emissions of mercury from municipal solid waste. II: potential losses of airborne mercury before landfill. J Air Waste Manage 55(7):870–877
Stein ED, Cohen Y, Winer AM (1996) Environmental distribution and transformation of mercury compounds. Crit Rev Env Sci Tec 26(1):1–43
Tao S, Deng B (1993) Content distribution pattern and pollution of mercury in soil from Shenzhen area. China Environ Sci 13(1):35–38 [in Chinese]
United Nations Environment Programme Chemicals (2002) Global mercury assessment. Switzerland. http://www.chem.unep.ch/mercury/Report/Final%20report/final-assessment-report-25nov02.pdf. Accessed December 2009
United States Environmental Protection Agency (1997) Mercury Study Report To Congress. EPA-452/R-97-005. http://www.epa.gov/hg/report.htm. Accessed December 2009
Wang DY, Qing CL, Guo TY, Guo YJ (1997) Effects of humic acid on transport and transformation of mercury in soil-plant systems. Water Air Soil Pollut 95(1–4):35–43
Wang DY, Shi XJ, Wei SQ (2003) Accumulation and transformation of atmospheric mercury in soil. Sci Total Environ 304(1–3):209–214
Xin M, Gustin MS (2007) Gaseous elemental mercury exchange with low mercury containing soils: investigation of controlling factors. Appl Geochem 22(7):1451–1466
Xin M, Gustin M, Johnson D (2007) Laboratory investigation of the potential for re-emission of atmospherically derived Hg from soils. Environ Sci Technol 41(14):4946–4951

Yang XP, Wang LQ (2008) Spatial analysis and hazard assessment of mercury in soil around the coal-fired power plant: a case study from the city of Baoji, China. Environ Geol 53(7): 1381–1388

Zemba SG, Green LC, Crouch EAC, Lester RR (1996) Quantitative risk assessment of stack emissions from municipal waste combustors. J Hazard Mater 47(1–3):229–275

Zhang H, Lindberg SE (1999) Processes influencing the emission of mercury from soils: a conceptual model. J Geophys Res Atmos 104(D17):21889–21896

Zhang H, Lindberg SE, Marsik FJ, Keeler GJ (2001) Mercury air/surface exchange kinetics of background soils of the Tahquamenon River watershed in the Michigan Upper Peninsula. Water Air Soil Poll 126(1–2):151–169